the linear heating times estimated for the present experiment give $\Delta T_e \lesssim 1$ eV/$\mu$sec near the upper hybrid frequency. The enhancement at the second harmonic is many orders of magnitude smaller. Since our measurements show (see Fig. 3) that under these conditions $\Delta T_e \simeq 20$–$30$ eV/$\mu$sec, and that very energetic particles are also produced within a microsecond ($U \lesssim 500$ eV), it is clear that linear theories do not explain our results. We believe that similar processes may occur in a number of experiments where heating near the upper hybrid or the cyclotron harmonics have been observed.[5,10] In contrast to recent heating experiments with frequencies below the electron cyclotron frequency where mainly heating of the tail of the distribution function was observed,[11] in the present case considerable heating of the main body of electrons was also observed. This is believed to be due to the strong interaction of the excited Bernstein waves with thermal electrons. Thus, heating at frequencies above the electron-cyclotron frequency may be more favorable for possible applications where fast heating of thermal electrons is desired.

*Work supported by the U. S. Atomic Energy Commission under Contract No. AT(11-1)-3073.

[1]R. A. Dandl *et al.*, Nucl. Fusion 11, 411 (1971).
[2]H. Ikegami, S. Aihara, and M. Hosokawa, Phys. Fluids 15, 2054 (1972).
[3]J. C. Sprott, K. A. Connor, and J. L. Shohet, Plasma Phys. 14, 269 (1972).
[4]O. Eldridge, Phys. Fluids 15, 676 (1972).
[5]V. V. Alikaev *et al.* Pis'ma Zh. Eksp. Teor. Fiz. 15, 41 (1972) [JETP lett. 15, 27 (1972)].
[6]R. P. H. Chang, M. Porkolab, and B. Grek, Phys. Rev. Lett. 28, 206 (1972).
[7]T. H. Stix, *Theory of Plasma Waves* (McGraw-Hill, New York, 1962), pp. 32, 41, 227, 244.
[8]S. Hiroe and H. Ikegami, Phys. Rev. Lett. 19, 1414 (1967). Note that in this work the wavelengths were not measured, and the thresholds were not compared with theory.
[9]M. Porkolab, Nucl. Fusion 12, 329 (1972).
[10]O. A. Anderson *et al.*, Bull. Amer. Phys. Soc. 17, 997 (1972).
[11]M. Porkolab, V. Arunasalam, and R. A. Ellis, Jr., Phys. Rev. Lett. 29, 1438 (1972).

## Rotation and Structure of Low-Frequency Oscillations inside the ST-Tokamak Plasma*

J. C. Hosea, F. C. Jobes, R. L. Hickok,† and A. N. Dellis‡
*Plasma Physics Laboratory, Princeton University, Princeton, New Jersey 08540*
(Received 26 February 1973)

Low-frequency oscillations, which can lead into the violent disruptive instability which sets the $q$ (current) limit of tokamak operation, are investigated with a heavy-ion beam probe. Direct measurements of the space potential and the perturbation of the electron density *inside* the hot tokamak plasma resolve the electric field contribution to the mode rotation and the spatial structure of the mode.

The two phases of magnetohydrodynamic (MHD) instability observed in tokamaks[1,2] appear conjointly; low-frequency, low-amplitude oscillatory modes with helical magnetic field perturbations [$B_\theta \propto \exp(im\theta - i\varphi)$] are observed to grow leading into the more deleterious "disruptive" instability characterized by a negative spike on the plasma loop voltage ($v_\varphi$) and a partial depletion of the energy stored in the plasma ($\theta$ and $\varphi$ are the minor and major azimuthal angles of the torus, respectively). As $m$ decreases, the intensity of the disruptive instability increases, until following $m = 2$, the disruptive instability dominates the tokamak discharge. In fact, the $m = 2$ oscillations are observed to precede the violent disruptive instabilities at both the low safety factor $q(a)$ and high-pressure (plasma density) limits to useful tokamak operation [$q(r) = rB_\varphi(R)/RB_\theta(r)$, where $r$ and $R$ are the minor and major toroidal radii, respectively, and $a$ is the plasma limiter radius]. Apparently, the disruptive instability occurs when the radial current distribution $j_\varphi(r)$ is such that the $q = m$ singular magnetic surface location is favorable to the enhanced growth of the $m$-mode oscillation.[1] (Runaway electrons do not appear to cause the instability.[3]) When the $q = 2$ singular surface is moved toward the plasma surface by lowering $q(a)$ or by causing the current channel to shrink by increasing pressure as evidenced by a constriction of the electron temperature profile,[1,4] the $m = 2$ mode grows to an amplitude of $\tilde{B}_\theta(d)/B_\theta(d) \sim 6\%$ at

which the violent instability ensues ($d = 16.9$ cm is the magnetic-probe position). [Of course, it is also possible that the $m = 1$ mode (Kruskal-Shafranov resistive kink[5-7]), as yet undetected, accounts for the violent instability since the $q = 1$ surface appears to be present simultaneously at a smaller radius than the $q = 2$ surface.]

In order to discern the true relationship of the disruptive instability to the oscillatory modes, as well as to evaluate the possible mode contributions to thermal and particle transport,[8] it is necessary to investigate the local properties of the instabilities inside the plasma, and especially in the vicinity of the singular surfaces. Consequently, we have extended our instability diagnosis to the *interior* of the plasma with a novel thallium-ion beam probe.[9] In this Letter, we present the first measurements of the plasma potential and the oscillatory-mode perturbation of the electron density profile inside the hot tokamak plasma. These data provide considerable insight into the mode properties and suggest that the ion-beam probe technique might indeed lead to the unambiguous identification of the oscillatory modes and the disruptive instability.

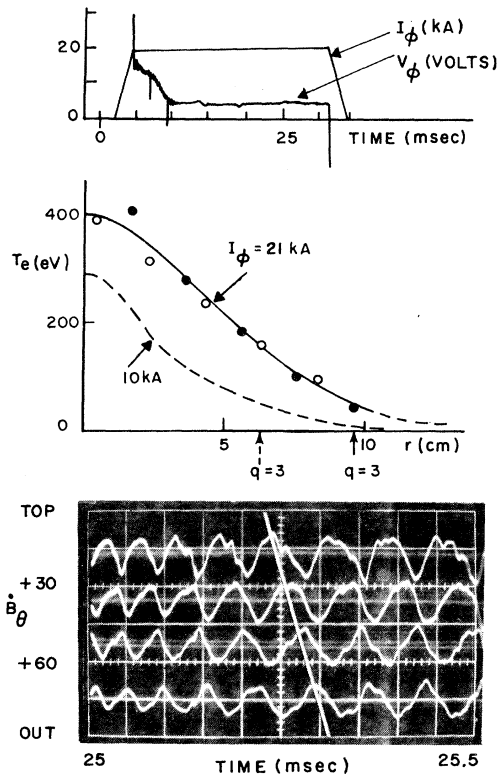


FIG. 1. Hydrogen discharge conditions investigated with the heavy-ion beam. [$B_\varphi = 14$ kG; limiter radius $a$, 10 cm; $B_\perp$ is adjusted to place the center of the plasma on the detector line, Fig. 3(a).] Laser temperature profiles are given for $t = 25$ msec and $I_\varphi = 21$ and 10 kA. The electron density profiles are identical with $n_e(0) = 1.6 \times 10^{13}$ cm$^{-3}$, and $m = 3$ oscillatory modes are monitored for both values of $I_\varphi$.

Representative discharge conditions for which we have employed the heavy-ion beam probe are illustrated in Fig. 1. $B_\varphi$, chosen commensurate with the beam accelerator potential (100 keV), is relatively low, but valid tokamak-type discharges are maintained. For both discharge currents, $I_\varphi = 21$ and 10 kA, typical ST temperature profiles are observed and the minimum energy containment times [(energy stored)/(power input)] are 1.6 and 1.4 msec, respectively. In both cases, $m = 3$ modes rotating in the electron diamagnetic drift direction are monitored with magnetic probes.

The singly ionized thallium primary ion beam ($I^+$) is injected at the top of the plasma column [several orbits are shown in Fig. 2(a)] and is ionized along its path according to

$$-dI^+ = I^+ n_e \langle \sigma_+ v_e \rangle dt = dI^{2+}. \quad (1)$$

An electrostatic analyzer, split-plate detector system[9] collects the doubly ionized secondary ion beam ($I^{2+}$) originating over a small length (~3 mm) of the primary beam in the vicinity of the detector line [Fig. 2(a)]. The secondary beam's intensity and energy, relative to those of the primary beam, and displacement in $\varphi$ are all monitored simultaneously. By sweeping the primary beam, these parameters are obtained as a function of position along the detector line

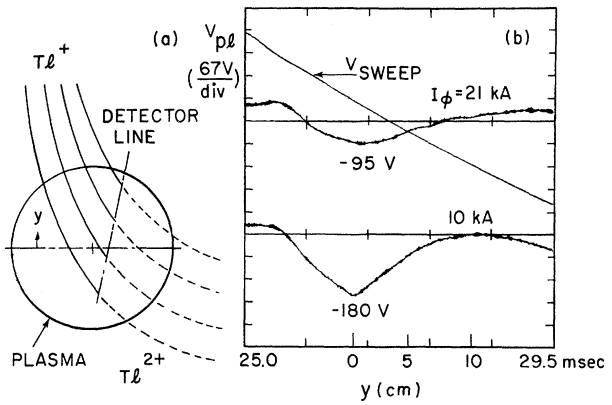


FIG. 2. Thallium-ion beam-probe measurements of the space potential. (a) Primary beam trajectories for different times during the sweep. (b) Space potential as a function of time during the sweep for the discharges of Fig. 1. The $y$ coordinate of the detector line is marked on the time axis.

over a relatively short period of time during a single discharge pulse. Therefore, the heavy-ion beam probe can measure, in principle, the radial profiles of electron density $n_e(r)$, plasma space potential $V_{pl}(r)$, and the current density $j_\varphi(r)$, as well as perturbations of these quantities by instabilities.

The first measurements of the space potential inside a tokamak plasma are presented in Fig. 2(b) for the discharge conditions of Fig. 1. These measurements apply to the detector line of Fig. 2(a) [which was located by first relating the primary beam position, detected with a probe, to the sweep voltage and then noting the peak in secondary beam intensity for a low-temperature, low-density, small-radius ($a = 6$ cm) plasma which was centered with respect to vertical position magnetic loops]. These space-potential profiles peak negatively at the center of the plasma column to sizable fractions of the peak electron temperatures (Fig. 1).

We may immediately use these new data to evaluate the contribution of the radial electric field to the oscillatory-mode frequency. We employ the oscillation model of Ref. 1, which assumes that the oscillations are produced by helical current filaments, centered on the rational $q = m$ magnetic surface, which rotate with the electrons at this singular surface. (This model is appropriately valid for the tearing- and drift-mode equilibria.) For this model the mode frequency $\omega$ is equal to the sum of the electron diamagnetic drift frequency $\omega^* = (m/B_\varphi r_m n_e)\partial(n_e T_e)/\partial r$ and the electric-field-driven rotation frequency $\omega_E = mE_r/B_\varphi r_m$:

$$\omega = \omega^* + \omega_E .$$

Table I gives $\omega_E$, calculated for the potential profiles [Fig. 2(b)], and $\omega^*$, calculated from the Thomson scattering measurements of $T_e$ and $n_e$, for the radii $r_3$ at which Eq. (2) is satisfied. [We find that $r_3$ agrees reasonably well with $r_{3L}$, the $q = 3$ surface location assuming $J_\varphi(r) \propto T_e^{3/2}$.]

TABLE I. $E_r$ and $V_r(n_e T_e)$ contributions to mode frequency for the conditions of Figs. 1 and 2. [Current, radii, and radian frequencies have units of kA, cm, and $10^4$ sec$^{-1}$, respectively.]

| $I_\varphi$ | $r_3$ | $\omega_E/3$ | $\omega^*/3$ | $\omega/3$ | $r_{3L}$ |
|---|---|---|---|---|---|
| 21 | 8.7 | 0.4 | 3.9 | 4.3 | 9.7 |
| 10 | 5.0 | 3.1 | 4.7 | 7.8 | 6.3 |

The $\omega_E$ term is much smaller than $\omega^*$ for $I_\varphi = 21$ kA but $\omega_E$ is comparable to $\omega^*$ for $I_\varphi = 10$ kA. Thus, the range in $\omega/\omega^*$ tabulated in Ref. 1 [$0.5 \lesssim \omega/\omega^* \lesssim 2.2$] can be explained, in part if not entirely, as due to the variation of the space-potential profile ($E_r$) with discharge conditions.

In the ST tokamak, the diamagnetic drift usually predominates, giving on the average $\omega/\omega^* \sim 1$. However, the antielectron diamagnetic drift of the modes observed in the T-3 tokamak would have necessitated a positive $E_r$ which outweighed the strong pressure gradient in the vicinity of the mode surface ($\nabla p$ is relatively weak only near the center of the plasma column[10]).

For the $I_\varphi = 21$-kA discharge of Fig. 1, a small perturbation was observed on the secondary beam intensity, which can be attributed to the electron density perturbation of the $m = 3$ mode [$\langle \sigma V_e \rangle$ of Eq. (1) is insensitive to $T_e$ for $T_e \gtrsim 80$ eV]. This perturbation peaked in the vicinity of $r = 9$ cm which is approximately the location of the $q = 3$ surface (Table I).

In order to enhance the density perturbation and to maintain a relatively constant oscillation (magnetic perturbation) amplitude during the sweep of the primary beam, we stepped the discharge current 10 msec prior to the start of the sweep. The resulting $Tl^{2+}$ intensity profile is given in Fig. 3. An annulus of density perturbation is clearly resolved. As the secondary beam sweeps up off of the exit duct it enters the lower region of density perturbation, passes through the central practically quiescent core, then through the upper region of density perturbation, and finally on out of the plasma column. (Modu-

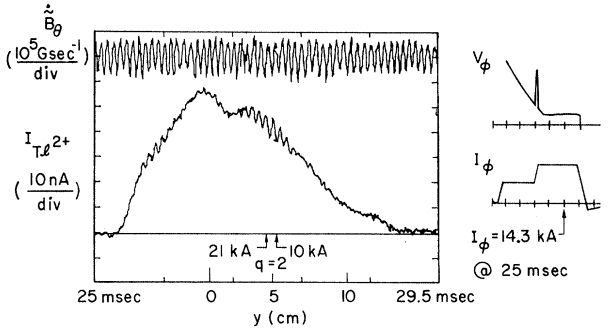


FIG. 3. Secondary beam intensity versus $y$ of the detector line showing the density perturbation by an $m = 2$ oscillation. A relatively uniform $\tilde{B}_\theta$ is observed over the sweep. (The other discharge conditions are as for Fig. 2.) The $q = 2$ surface positions for $j_\varphi(r) \propto T_e^{3/2}$ are indicated for the constant-current discharges of Fig. 2.

lation of the primary beam as it passes through the annulus accounts for the very small secondary beam oscillations in the core.)

The oscillatory appearance of the density perturbation is caused by the slow sweep of the beam (~4 msec) relative to the period ($\tau \sim 0.09$ msec) of the $m = 2$ oscillation (plasma rotation). Expanded recordings reveal that the density oscillations have the proper phase relative to the magnetic probe signal; the density perturbations on opposite sides of the plasma are in phase. (For different conditions, $m = 3$ modes give the expected phase reversal.) Also, the measured density perturbation exhibits essentially no radial shear. This observation combined with the rotation results suggests a refined oscillation model for which the density perturbation rotates in a rigid rotor fashion along with the localized helical current filaments.

The maximum density perturbation in Fig. 3 is $\sim \pm 9\%$ (compatible with the modulation of the average $n_e$ measured with a 4-mm microwave interferometer) and occurs at $r \sim 6$ cm, well inside the limited radius $a = 10$ cm. This radius falls in the vicinity of the $q = 2$ singular magnetic-surface locations for the temperature profiles of Fig. 1 [assuming $j_\varphi(r) \propto T_e^{3/2}$]. [The skin time is much shorter than the 10 msec allowed in Fig. 3 for the temperature (current) profile to relax back to its usual shape.[12]] Surprisingly, there is no phase reversal of the density perturbation at the supposed $q = 2$ surface location as predicted by the linear resistive MHD theory.[13,14] Perhaps the $q = 2$ surface is maintained at a larger radius by the $m = 2$ mode itself. (When the current is raised to 14.3 at the start of the discharge, only the $m = 3$ mode is observed.) There is a hint of a phase reversal in Fig. 3 for $r \gtrsim 8$ cm ($y \gtrsim 7$ cm). However, it may result that the eigenmode which peaks at the singular surface is preferred in these plasmas.[14] Clearly, we must await the perfection of the direct measurement of $j_\varphi(r)$ in order to resolve the exact phase relationship.

The mode of Fig. 3 is found not to be a surface mode and is therefore of the resistive type (the $m = 2$ flute mode is shear stabilized[15]). Therefore, the most likely cause of the oscillation is a form of the tearing mode.[7] However, further experimental study and theoretical analyses of more appropriate rotaring plasma models are needed to make a more definitive designation.

If it should result that the $m = 2$ mode does cause the violent disruptive instability, it would then be desirable to stabilize this oscillatory mode with feedback or dynamic stabilization. Since the mode location is well inside the plasma, dynamic stabilization appears to be preferable (e.g., supplementary heating in the outer region of the plasma column).

We wish to express our appreciation to Dr. C. Bobeldijk for his valuable assistance in the initial phase of this experiment, to Dr. D. Dimock and Dr. L. Johnson for providing the illuminating laser scans used in this study, and to Professor P. Rutherford and Professor H. Furth for many informative discussions.

---

*Work supported by U.S. Atomic Energy Commission under Contract No. AT(11-1)-3073 and by U.S. Air Force Office of Scientific Research Grant No. 72-2191.

†Permanent address: Renssalaer Polytechnic Institute, Troy, N.Y. 12181.

‡Permanent address: United Kingdom Atomic Energy Authority Research Group, Culham Laboratory, England.

[1]J. C. Hosea, C. Bobeldijk, and D. J. Grove, in *Proceedings of the Fourth International Conference on Plasma Physics and Controlled Nuclear Fusion Research, Madison, Wisconsin, 1971* (International Atomic Energy Agency, Vienna, 1972), Vol. II, p. 425.

[2]S. V. Mirnov and I. B. Semenov, At. Energ. 30, 14 (1971) [Sov. At. Energy 30, 14 (1971)].

[3]S. von Goeler *et al.*, Bull. Amer. Phys. Soc. 16, 1231 (1971).

[4]Princeton Plasma Physics Laboratory Report No. MATT-Q-29, 1971 (unpublished), Fig. 17.

[5]L. A. Artsimovich *et al.*, Nucl. Fusion Special Suppl. 17 (1969).

[6]V. D. Shafranov, Zh. Tekh. Fiz. 40, 241 (1970) [Sov. Phys. Tech. Phys. 15, 175 (1970)].

[7]P. H. Rutherford, H. P. Furth, and M. N. Rosenbluth, in *Proceedings of the Fourth International Conference on Plasma Physics and Controlled Nuclear Fusion Research, Madison, Wisconsin, 1971* (International Atomic Energy Agency, Vienna, 1971), Vol. II, pp. 553–570.

[8]S. V. Mirnov, Nucl. Fusion 9, 57 (1969).

[9]R. L. Hickok and F. C. Jobes, U.S. Air Force Office of Scientific Research No. TR-72-0018, 1972 (unpublished), pp. 53–57, and Nucl. Fusion 10, 195 (1970).

[10]N. J. Peacock *et al.*, Nature (London) 224, 488 (1969).

[11]J. C. Hosea and F. C. Jobes, to be published.

[12]C. Bobeldijk, D. Dimock, and J. C. Hosea, Bull. Amer. Phys. Soc. 16, 1232 (1971).

[13]H. P. Furth, J. Killeen, and M. N. Rosenbluth, Phys. Fluids 6, 459 (1963).

[14]B. Coppi, J. M. Greene, and J. L. Johnson, Nucl. Fusion 6, 101 (1966).

[15]V. D. Shafranov, Nucl. Fusion 8, 253 (1968).

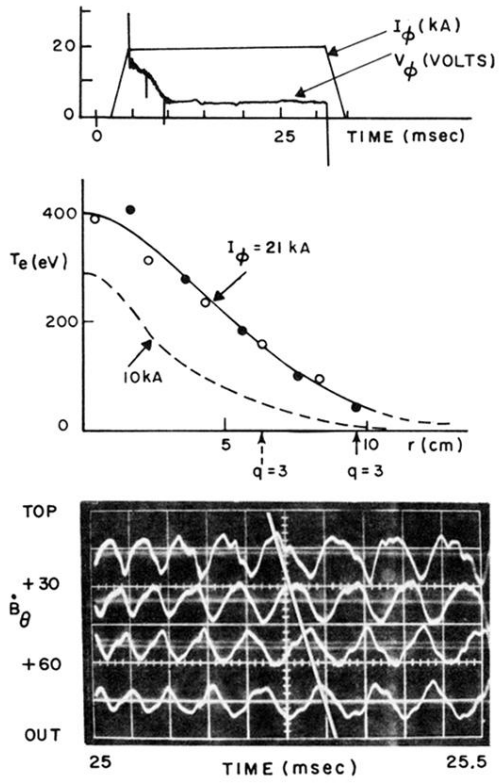


FIG. 1. Hydrogen discharge conditions investigated with the heavy-ion beam. [$B_\varphi = 14$ kG; limiter radius $a$, 10 cm; $B_\perp$ is adjusted to place the center of the plasma on the detector line, Fig. 3(a).] Laser temperature profiles are given for $t = 25$ msec and $I_\varphi = 21$ and 10 kA. The electron density profiles are identical with $n_e(0) = 1.6 \times 10^{13}$ cm$^{-3}$, and $m = 3$ oscillatory modes are monitored for both values of $I_\varphi$.